Corresponding Author: Dr. Kyung-Duck Suh, PhD

Corresponding Author's Institution: Seoul National University

First Author: Tae-Hwa Jung, MS

Order of Authors: Tae-Hwa Jung, MS; Kyung-Duck Suh, PhD

Manuscript Region of Origin:

Abstract: An analytic solution to the mild slope equation is derived for waves propagating over an axi-symmetric pit located in an otherwise constant depth region. The water depth inside the pit decreases in proportion to an integer power of radial distance from the pit center. The mild slope equation in cylindrical coordinates is transformed into ordinary differential equations by using the method of separation of variables, and the coefficients of the equation in radial direction are transformed into explicit forms by using the direct solution for the wave dispersion equation by Hunt (Hunt, J.N., 1979. Direct solution of wave dispersion equation. J. Waterw., Port, Coast., Ocean Div., Proc. ASCE, 105, 457-459). Finally, the Frobenius series is used to obtain the analytic solution. Due to the feature of the Hunt's solution, the present analytic solution is accurate in shallow and deep waters, while it is less accurate in intermediate depth waters. The validity of the analytic solution is demonstrated by comparison with numerical solutions of the hyperbolic mild slope

equations. The analytic solution is also used to examine the effects of the pit geometry and relative depth on wave transformation. Finally, wave attenuation in the region over the pit is discussed.

Cover Letter

San 56-1, Shillim-Dong, Gwanak-Gu,
Seoul 151-744, Korea
Tel: +82-2-880-8760
Fax: +82-2-887-0349

Department of Civil, Urban, and Geosystem Engineering
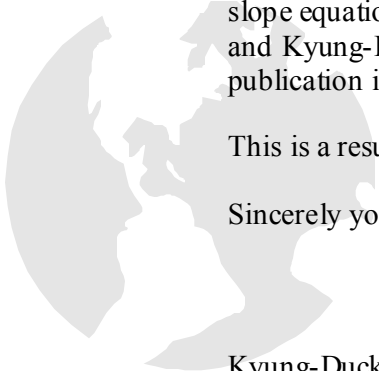# Seoul National University

November 10, 2006

To whom it may concern:

Please find the enclosed manuscript entitled "An analytic solution to the mild slope equation for waves propagating over an axi-symmetric pit" by Tae-Hwa Jung and Kyung-Duck Suh. I would like to have the manuscript reviewed for possible publication in Coastal Engineering.

This is a resubmission.

Sincerely yours,

Kyung-Duck Suh, Ph.D.
Professor
Department of Civil, Urban and Geosystem Engineering
Seoul National University
E-mail: kdsuh@snu.ac.kr

An analytic solution to the mild slope equation for waves propagating over an axi-symmetric pit

Tae-Hwa Jung[a], Kyung-Duck Suh[b,*]

[a] *School of Civil, Urban, and Geosystem Engineering, Seoul National University, Seoul 151-744, South Korea*

[b] *School of Civil, Urban, and Geosystem Engineering & Engineering Research Institute, Seoul National University, Seoul 151-744, South Korea*

Abstract

An analytic solution to the mild slope equation is derived for waves propagating over an axi-symmetric pit located in an otherwise constant depth region. The water depth inside the pit decreases in proportion to an integer power of radial distance from the pit center. The mild slope equation in cylindrical coordinates is transformed into ordinary differential equations by using the method of separation of variables, and the coefficients of the equation in radial direction are transformed into explicit forms by using the direct solution for the wave dispersion equation by Hunt (Hunt, J.N., 1979. Direct solution of wave dispersion equation. J. Waterw., Port, Coast., Ocean Div., Proc. ASCE, 105, 457-459). Finally, the Frobenius series is used to obtain the analytic solution. Due to the feature of the Hunt's solution, the present analytic solution is accurate in shallow and deep waters, while it is less accurate in intermediate depth waters. The validity of the analytic solution is demonstrated by comparison with numerical solutions of the hyperbolic mild slope equations. The analytic solution is also used to examine the effects of the pit geometry and relative depth on wave transformation. Finally, wave attenuation in the region over the pit is discussed.

Keywords: analytic solution; axi-symmetric pit; mild slope equation; wave transformation

---

[*] Corresponding author. Tel.: +82 2 880 8760; fax: +82 2 887 0349.
E-mail addresses: togye176@snu.ac.kr (T.-H. Jung), kdsuh@snu.ac.kr (K.-D. Suh)

1. Introduction

As surface gravity waves propagate from deep to shallow water, they are transformed by refraction, diffraction, shoaling, and reflection until they break and dissipate. Numerous numerical models have been developed to predict the transformation of waves. Many of them are based on the mild slope equation, which has been used for various linear water wave problems since first proposed by Berkhoff (1972). However, since numerical models inherently involve approximations, it is necessary to test these models against analytic solutions and/or laboratory and field experiment data. Experimental data may be preferred since they are the physical systems of interest, but they are expensive and time-consuming to obtain. Also, experimental data always contain a certain amount of measurement errors. An advantage of analytic solutions is that they are generally developed at reduced cost, time, and labor in comparison to experiments. Nonetheless, most wave transformation problems are complex, and analytic solutions are available for only special situations.

A frequently considered problem in analytic studies of wave transformation is the long wave motion around a circular island mounted on an axi-symmetric shoal. Homma (1950), Vastano and Reid (1967), Jonsson et al. (1976), and Zhu and Zhang (1996) studied long waves around a circular island situated on a parabolic or conical shoal. Recently, Yu and Zhang (2003) presented a more general solution by describing the radial topography of the shoal by a power of the radial distance. More recently, Liu et al. (2004) extended the Homma's solution to intermediate depth water waves by using Hunt's (1979) approximate direct solution of the implicit wave dispersion equation to explicitly express the coefficients of the mild slope equation.

On the other hand, Suh et al. (2005) presented an analytic solution for long waves propagating over an axi-symmetric pit where the water depth decreases from the center to the edge in proportion to the second power of the radial distance from the pit center. In the present study, first, the restriction on topography in Suh et al.'s solution is eased by making the water depth inside the pit vary in proportion to any integer power of the radial distance; the first power corresponds to a conical pit and the pit approaches to a cylindrical pit as the power increases. Second, Suh et al.'s solution is extended to deeper waters by using Hunt's (1979) direct solution for the wave dispersion equation as done by Liu et al. (2004). In the following section, we derive an analytic solution to the mild slope equation for waves propagating over an axi-symmetric pit. The analytic solution is then compared with Suh et al.'s (2005) long wave solution and a numerical solution based on the

hyperbolic form of the mild slope equation. We also discuss the effects of the pit geometry on the wave scattering using our analytic solution. Finally, wave attenuation in the region over the pit is discussed, and then we summarize the major conclusions.

2. Analytic solution

Consider an axi-symmetric pit situated in an otherwise constant depth region as shown in Fig. 1, where the origin of the horizontal coordinate system is taken to be the center of the pit, r is the radial distance from the origin, and θ is the angle measured counterclockwise from the positive x-axis. The incident wave is assumed to be a long-crested wave propagating in the positive x-direction. The water depths at the origin and in the constant depth region are denoted by h_0 and h_1, respectively. The water depth in the pit is assumed to decrease from the center to the edge, according to the law, $h = h_0(1 - r^\alpha / a^\alpha)$, where a is the radial distance from the pit center to the imaginary edge of the pit extended to the water surface and the power α is a positive integer. Denoting the radial distance to the actual edge of the pit as b, the water depth is given by

$$h = \begin{cases} h_0\left(1 - \dfrac{r^\alpha}{a^\alpha}\right) & r < b \\[3mm] h_1 = h_0\left(1 - \dfrac{b^\alpha}{a^\alpha}\right) & r \geq b \end{cases} \tag{1}$$

Fig. 2 shows the water depth along the x-axis for various values of α. The pit has a conical shape for $\alpha = 1$, and the pit approaches to a cylindrical pit with a vertical side slope as α increases.

The mild slope equation for combined refraction and diffraction is given by

$$\nabla \cdot (CC_g \nabla \eta) + \sigma^2 \frac{C_g}{C} \eta = 0 \tag{2}$$

where η is the complex water surface elevation, C is the phase speed, C_g is the

group velocity, σ is the wave angular frequency, and ∇ is the horizontal gradient operator. In the pit area where $h = h(r)$, this equation can be expressed in cylindrical coordinates as

$$CC_g \frac{\partial^2 \eta}{\partial r^2} + \frac{d(CC_g)}{dr} \frac{\partial \eta}{\partial r} + \frac{1}{r} CC_g \frac{\partial \eta}{\partial r} + \frac{1}{r^2} CC_g \frac{\partial^2 \eta}{\partial \theta^2} + \sigma^2 \frac{C_g}{C} \eta = 0 \tag{3}$$

To solve the preceding equation analytically, Hunt's (1979) approximate direct solution of the implicit wave dispersion equation is used as follows:

$$(kh)^2 = \nu^2 + \frac{\nu}{P(\nu)} \tag{4}$$

$$P(\nu) = 1 + \frac{2}{3}\nu + \frac{16}{45}\nu^2 + \frac{152}{945}\nu^3 + \frac{896}{14175}\nu^4 + \cdots \tag{5}$$

where $\nu = \sigma^2 h / g$, k is the wave number, and g is the gravitational acceleration. For convenience, we denote $P(\nu) = \sum_{j=0}^{s} d_j \nu^j$ with $d_0 = 1$, and the corresponding direct solution will be called Hunt's s th order approximate solution. Hunt's solution, if its order is greater than or equal to two, satisfies the asymptotic dispersion relationships in both deep and shallow waters, i.e., $\sigma^2 = gk$ as $\nu \to \infty$ and $\sigma^2 = gk^2 h$ as $\nu \to 0$. The phase speeds for different orders of Hunt's solution, normalized with respect to the linear-theory phase speed, are plotted as a function of ν in Fig. 3. Although Hunt's solution approaches the solution of the linear dispersion equation as the order increases, it is not possible to analytically judge the convergence of the Frobenius series, which is used later to derive the analytic solution, if the order is greater than or equal to five. It is possible to judge the convergence numerically for higher orders of Hunt's solution using Bairstow's method (see Press et al., 1992, p. 370), for example. However, the analytic solution becomes much more complicated as the order increases. Therefore, the Hunt's 4th order solution is used in this study. In this case, the relative error in the calculation of the phase speed is less than 1% for all values of ν as shown in Fig. 3.

Using Eq. (4), the coefficients in Eq. (3), i.e., CC_g, C_g / C, and $d(CC_g)/dr$, can be expressed as explicit functions:

4

$$CC_g \approx \frac{g^2}{2\sigma^2}\frac{v(P(v)+1)}{P(v)v+1} \tag{6}$$

$$\frac{C_g}{C} \approx \frac{P(v)+1}{2P(v)} \tag{7}$$

$$\frac{d(CC_g)}{dr} \approx \frac{g}{2}\frac{3(P(v)+1)-2(P(v)v+1)}{(P(v)v+1)(P(v)+1)}\frac{dh}{dr} \tag{8}$$

Substituting Eqs. (6) to (8) into Eq. (3) yields the following approximate form of the mild slope equation

$$g^2 P(v)v[P(v)+1]^2 r^2 \frac{\partial^2 \eta}{\partial r^2}$$

$$+ g\sigma^2 P(v)\{3[P(v)+1]-2[P(v)v+1]\}r^2 \frac{dh}{dr}\frac{\partial \eta}{\partial r} + g^2 P(v)v[P(v)+1]^2 r\frac{\partial \eta}{\partial r} \tag{9}$$

$$+ g^2 P(v)v[P(v)+1]^2 \frac{\partial^2 \eta}{\partial \theta^2} + \sigma^4 [P(v)v+1][P(v)+1]^2 r^2 \eta = 0$$

Using the method of separation of variables, the solution to Eq. (9) can be expressed as

$$\eta_1(r,\theta) = \sum_{n=0}^{\infty} R_n(r)\cos n\theta \tag{10}$$

where the subscript 1 denotes the inside of the pit, i.e., $r < b$, and the terms associated with $\sin n\theta$ have been dropped based on the symmetry condition about the x-axis. The function $R_n(r)$ takes the form of a Frobenius series:

$$R_n(r) = \sum_{m=0}^{\infty} a_{m,n} r^{m+c} \tag{11}$$

Substituting Eqs. (1) and (10) into Eq. (9) yields a second-order ordinary differential equation for $R_n(r)$ with variable coefficients, which, using Eq. (11), can be expressed as

$$A(r)\sum_{m=0}^{\infty}a_{m,n}(m+c)(m+c-1)r^{m+c}+B(r)\sum_{m=0}^{\infty}a_{m,n}(m+c)r^{m+c}$$
$$+\{C(r)-n^2D(r)\}\sum_{m=0}^{\infty}r^{m+c}=0 \tag{12}$$

The variable coefficients $A(r)$, $B(r)$, $C(r)$, and $D(r)$ are given in Appendix A.

The indicial equation to calculate the value of c in Eq. (12) becomes

$$A_1c(c-1)r^c+B_1cr^c-n^2D_1r^c=0 \tag{13}$$

Since A_1, B_1, and D_1 are all the same, we obtain $c=\pm n$, which, in turn, give two linearly independent solutions:

$$R_{n,1}=\sum_{m=0}^{\infty}a_{m,n}r^{m+n} \tag{14}$$

$$R_{n,2}=R_{n,1}\ln r+\sum_{m=0}^{\infty}b_{m,n}r^{m-n} \tag{15}$$

Imposing the condition that water surface elevation must be finite at the origin, $R_{n,2}$ can be omitted. Substituting Eq. (14) into Eq. (12) and collecting the terms of the same order of r, we obtain the recurrence relations for $a_{m,n}$, which are given in Appendix B. Finally, the water surface elevation inside the pit can be written as follows:

$$\eta_1=\sum_{n=0}^{\infty}A_nR_n\cos n\theta \tag{16}$$

where A_n is a set of complex constants to be determined.

In order to obtain the full solution, we apply the method of matched eigen-expansions. Accordingly, we divide the fluid domain into two regions in the horizontal plane: the finite region with variable depth ($r<b$) and the semi-infinite far region with constant depth ($r\geq b$). In the far region, the water surface elevation can be obtained as the sum of the long-crested incident wave propagating in the positive x-direction and the scattered wave

6

satisfying the Sommerfeld radiation condition at infinity. Again imposing the symmetry condition about the x-axis, the water surface elevation in the far region can be written as

$$\eta_2 = \sum_{n=0}^{\infty}[a_i i^n \varepsilon_n J_n(kr) + D_n H_n^{(1)}(kr)]\cos n\theta \qquad (17)$$

where a_i is the incident wave amplitude, $i = \sqrt{-1}$, J_n is the Bessel function of the first kind of order n, $H_n^{(1)}$ is the Hankel function of the first kind of order n, and D_n is a set of complex constants to be determined. ε_n is the Jacobi symbol defined by

$$\varepsilon_n = \begin{cases} 1, & n = 0 \\ 2, & n \geq 1 \end{cases} \qquad (18)$$

At $r = b$, the dynamic and kinematic matching conditions require

$$\eta_1 = \eta_2 \qquad \text{at } r = b \qquad (19)$$

$$\frac{\partial \eta_1}{\partial r} = \frac{\partial \eta_2}{\partial r} \qquad \text{at } r = b \qquad (20)$$

respectively. Substituting Eqs. (16) and (17) into Eqs. (19) and (20) while noting that $\{\cos n\theta\}$ form an orthogonal set, we find

$$A_n = a_i k i^n \varepsilon_n \frac{J_n(kb)H_n^{(1)\prime}(kb) - J_n'(kb)H_n^{(1)}(kb)}{kR_n(b)H_n^{(1)\prime}(kb) - R_n'(b)H_n^{(1)}(kb)} \qquad (21)$$

$$D_n = a_i i^n \varepsilon_n \frac{kJ_n'(kb)R_n(b) - J_n(kb)R_n'(b)}{H_n^{(1)\prime}(kb)R_n'(b) - kH_n^{(1)\prime}(kb)R_n(b)} \qquad (22)$$

where the prime denotes derivatives. Substituting these coefficients back into Eqs. (16) and (17), we can compute the water surface elevation for the whole domain.

3. Results and discussions

3.1. Convergence of solution

The convergence of the Frobenius series is dependent upon the behavior of the first variable coefficient in Eq. (9), i.e., $P(v)v[P(v)+1]^2 r^2$. The least convergent radius is from the expanding point ($r = 0$ in our case) to the nearest singular point. The singular points are calculated by the root of $P(v)v[P(v)+1]^2 r^2 = 0$ as

$$r = 0, \ a \tag{23}$$

$$r = \sqrt[\alpha]{a^\alpha + \frac{1.63009 \pm 1.10252i}{\delta}} \tag{24}$$

$$r = \sqrt[\alpha]{a^\alpha - \frac{0.357769 \pm 1.98923i}{\delta}} \tag{25}$$

$$r = \sqrt[\alpha]{a^\alpha + \frac{1.9903 \pm 1.55755i}{\delta}} \tag{26}$$

$$r = \sqrt[\alpha]{a^\alpha - \frac{0.717978 \pm 2.10671i}{\delta}} \tag{27}$$

where $\delta = \sigma^2 h_0 / g a^\alpha$.

$r = 0$ in Eq. (23) is excluded because it is the expanding point of the Frobenius series in this study. Since δ is positive, the values of r in Eqs. (23), (24), and (26) are all greater than or equal to a. In Eqs. (25) and (27), r varies depending on δ, having the minimum value of $r = 0.94655a$ at $\delta = 0.69$ in the case of $\alpha = 1$ (Note that the minimum value of r increases with α, thus $\alpha = 1$ gives the smallest convergence radius). Because the Frobenius series is used in the range of $0 \le r < b$, the convergence is guaranteed if $b < 0.94655a$. Due to the relation of $b = a\sqrt[\alpha]{1 - h_1/h_0}$, h_1/h_0 must be much smaller than 1 for the series to diverge, i.e., for $b \ge 0.94655a$. However, this occasion is very rare, and the mild slope equation is not useful in such an occasion because the bottom slope near the edge of the pit is very large. Therefore, it can be said that the Frobenius series converges in the area where the mild slope equation is applicable.

The analytic solution for η involves an infinite eigenfunction series, but in practice

it must be properly truncated. In other words, we must find an integer N that is large enough such that the infinite series in Eqs. (16) and (17) is approximated with the desired accuracy. Numerical tests showed that $N = 70$ was enough to give accurate results for the power less than about 20. As the power increases, however, a larger N should be used. The number of terms, M, of the truncated Frobenius series of Eq. (14) should also be large enough to give accurate results. It was shown that the value of M required for the convergence of the Frobenius series increases with the radial distance r. In this study, therefore, with $N = 70$ fixed, M was determined for $r = b$ and $n = 70$ such that

$$\frac{\left| a_{M,70} b^{M+70} \right|}{\left| \sum_{m=0}^{M} a_{m,70} b^{m+70} \right|} < 10^{-5} \tag{28}$$

is satisfied. This M was then used for the calculation of R_n or $R_n^{'}$ in Eqs. (21) and (22).

3.2. Comparison with other analytic and numerical solutions

For comparison, the analytic solution for the case of $\alpha = 2$ was compared with Suh et al.'s (2005) long wave solution and the numerical solution based on the hyperbolic mild slope equations developed by Copeland (1985). See Suh et al. (2001) for more details of the computational procedure used for hyperbolic mild slope equation models. For the numerical solution, the grid spacing was chosen to be $\Delta x = \Delta y = L_1 / 30$, where L_1 is the wavelength in the constant depth region. The time step was chosen for the Courant number $C_r = C_1 \Delta t / \Delta x$ to be 0.1, where C_1 is the wave phase speed in the constant depth region. The incident waves were generated inside the model domain using the so-called internal wave generation technique. Sponge layers were used at both upwave and downwave boundaries, and reflecting conditions at the side boundaries. The analytic solution was computed from $-4L_1$ to $4L_1$ in the lateral direction. However, the numerical computation was performed from $-8L_1$ to $8L_1$ and only the results in the range of $-4L_1$ to $4L_1$ were used, in which the effect of the side boundaries was minimal. The constant water depth, h_1, was 3.2 m, and the water depth at the center of the pit, h_0, was 6.4 m. The dimensionless radius of the pit was $b/L_1 = 0.5$. We tested three different

relative depths in the constant depth region, $k_1 h_1$: 0.083, 0.334, and 1.336. The corresponding relative depths at the center of the pit, $k_0 h_0$, were 0.118, 0.481, and 2.368, respectively. The first case satisfies the common criterion for long waves, $kh \leq \pi/10$, in the entire area, while the second one slightly violates the long wave criterion. In the third case, the waves are in intermediate depth water in the entire area.

Figs. 4 to 6 compare the diffraction coefficients (i.e. the wave amplitude relative to the incident amplitude) among the solutions along the x-axis and y-axis for different relative depths. The results are presented in terms of dimensionless coordinates, x/L_1 and y/L_1. In Fig. 4 where the long wave criterion is satisfied, all the analytic and numerical solutions are almost identical except in the far downwave region, where the numerical solution exhibits some disturbance probably due to small wave reflection from the downwave sponge layer. In Fig. 5 where the long wave criterion is slightly violated, the present solution and the numerical solution are almost identical, while Suh et al.'s (2005) solution assuming long waves shows slight difference. In Fig. 6 where the waves are in intermediate depth water, the present solution shows good agreement with the numerical solution, while Suh et al.'s solution shows a quite different behavior as expected. It can be seen that in front of the pit a partial standing wave system develops, while in the lee of the pit a shadow zone exists in which wave heights are reduced. A small peak of diffraction coefficient appears just in front of the rear end of the pit, i.e. at $x/L_1 \cong 0.4$, in relatively shallow waters, probably due to wave reflection from the rear wall of the pit. This peak disappears in intermediate depth water as shown in Fig. 6. As the relative depth increases, both reflection and refraction of waves by the pit decrease so that there is less reduction of wave heights behind the pit. In the lateral direction, the diffraction coefficient shows a depression at the center of the pit in relatively shallow waters, but the depression disappears in intermediate depth water.

3.3. Effects of pit geometry

Figs. 7 and 8 show diffraction coefficients along the x-axis and y-axis for the cases of h_0 = 6.4, 9.6, and 12.8 m with a pit radius of $b = 0.5L_1$ for two different relative depths, $k_1 h_1 = 0.167$ and 1.336. $\alpha = 2$ and $h_1 = 3.2$ m were used. As the depth of the pit increases, the partial standing wave (due to reflection) in front of the pit increases, and more wave energy is also scattered laterally due to refraction; thus, there is more of a reduction of wave heights in the shadow zone. The location of the smallest wave height in the shadow zone is shifted backwards as the depth of the pit increases, but the location of

the small peak in the pit remains almost constant in the case of shallow water ($k_1 h_1 = 0.167$). The lateral variation of the diffraction coefficient also increases with the depth of the pit, showing the locations of its maxima and minima be shifted farther from the pit as the pit depth increases, though the shift is minimal in the intermediate depth water.

Figs. 9 and 10 show diffraction coefficients along the x- and y-axis for the cases of b/L_1 = 0.25, 0.5, 0.75, and 1.0 with a pit depth of h_0 = 6.4 m for two different relative depths, $k_1 h_1 = 0.167$ and 1.336. Again $\alpha = 2$ and $h_1 = 3.2$ m were used. As the pit radius increases with respect to the maximum depth, the slope within the pit decreases, hence, less wave reflection occurs. However, the effect of the increased refractive scattering of the larger pits is greater; thus, for larger pits there is still a greater reduction of wave heights in the shadow zone. The location of the smallest wave height in the shadow zone is shifted backwards as the radius of the pit increases. In the case of shallow water, the location of the small peak in the pit is also shifted backwards as the pit radius increases, because the real wall of the pit is shifted backwards. As with the pit depth, the lateral variation increases with the radius of the pit. Again as expected, the locations of maxima and minima of the diffraction coefficient are shifted farther from the pit as the radius increases, especially in shallow water.

Figs. 11 and 12 show diffraction coefficients along the x- and y-axis for the cases of α = 1, 2, 4, and 8 with h_0 = 6.4 m, $h_1 = 3.2$ m, and $b = 0.5L_1$ for two different relative depths, $k_1 h_1 = 0.167$ and 1.336. As α increases, the slope within the pit increases, so that the partial standing wave (due to reflection) in front of the pit increases and more energy is also scattered laterally due to refraction; thus, there is more of a reduction of wave heights in the shadow zone. The location of the smallest wave height in the shadow zone is shifted backwards as α increases, but the location of the small peak in the pit remains almost constant in the case of shallow water ($k_1 h_1 = 0.167$). The lateral variation of the diffraction coefficient also increases with α, showing the locations of its maxima and minima be shifted farther from the pit as α increases. It is noticeable that a new local peak starts to appear near the upwave boundary of the pit (i.e., $x \cong -0.4L_1$) as α increases, probably due to re-reflection of the waves from the steeper upwave slope of the pit.

3.4. Wave attenuation inside pits

When long waves propagate over a submerged island or shoal, waves are trapped in the region over the island so that the amplitude of each wave mode is amplified at the resonant frequencies (see Longuet-Higgins (1967) and Liu (1986)). On the other hand, in

the case of a parabolic pit ($\alpha = 2$), Suh et al. (2005) showed that wave attenuation occurred in such a way that the wave amplitude became smaller than the incident amplitude in the region over the pit. Fig. 13 shows the amplitudes of the first wave modes ($n = 0$) in the region over the pit relative to the incident amplitude as a function of the dimensionless frequency, $b\sigma / \sqrt{gh_0}$, for different values of α. The geometry of the pit is the same as that used to produce Fig. 11. The dimensionless amplitudes are unity for very long waves, decreasing to the dimensionless frequency of about 2 to 2.5, and bouncing to oscillate around 0.75 for larger frequencies. The oscillation is amplified with the power, α. Without showing the results, we mention that the amplitudes of the higher modes being very small for very long waves increase monotonically with the frequency, but they are much smaller than that of the first wave mode. In conclusion, wave attenuation occurs in the region over the pit with greater variation with frequency for larger α.

4. Conclusion

We derived an analytic solution to the mild slope equation for waves propagating over an axi-symmetric pit located in an otherwise constant depth region. The coefficients of the mild slope equation, which are transcendental functions, were expressed as explicit functions, by using Hunt's (1979) direct solution to the implicit wave dispersion equation. The mild slope equation in cylindrical coordinates was then solved by using the method of separation of variables and method of Frobenius.

It was shown that the Frobenius series used in this study converges unless the bottom slope is so large that the mild slope equation cannot be used. The present analytic solution was compared with a previously developed long wave solution and a finite-difference solution of the hyperbolic mild slope equations in the case of a parabolic pit ($\alpha = 2$). All the solutions were almost identical when the long wave criterion was satisfied. In intermediate depth water, however, the long wave solution showed a quite different behavior as expected, while the present solution and the numerical solution were in good agreement. The present solution will be accurate in deep water since the error of Hunt's solution decreases with water depth as shown in Fig. 1, though the bottom effects on surface waves are negligible there. Hence, the present solution represents a rigorous test case for numerical implementations of the mild slope equation regardless of water depth.

The effects of the pit geometry such as the central depth, radius of the pit, and the shape of the pit were also examined, and the variation in wave scattering for different pit configurations was described. Finally, the wave attenuation in the region of the pit was described.

Acknowledgments

Appendix A. Variable coefficients

$$
\begin{aligned}
A(r) &= P(v)(a^{\alpha} - r^{\alpha})[P(v)+1]^2 \\
&= A_1 + A_2 r^{\alpha} + A_3 r^{2\alpha} + A_4 r^{3\alpha} + A_5 r^{4\alpha} + A_6 r^{5\alpha} + A_7 r^{6\alpha} + A_8 r^{7\alpha} \\
&\quad + A_9 r^{8\alpha} + A_{10} r^{9\alpha} + A_{11} r^{10\alpha} + A_{12} r^{11\alpha} + A_{13} r^{12\alpha} + A_{14} r^{13\alpha}
\end{aligned} \tag{29}
$$

$$
\begin{aligned}
A_1 &= 4a^{\alpha} + 5.333333333 a^{2\alpha}\varepsilon + 5.066666667 a^{3\alpha}\varepsilon^2 + 3.953439153 a^{4\alpha}\varepsilon^3 \\
&\quad + 2.684162257 a^{5\alpha}\varepsilon^4 + 1.460599647 a^{6\alpha}\varepsilon^5 + 0.7120929425 a^{7\alpha}\varepsilon^6 \\
&\quad + 0.3043151834 a^{8\alpha}\varepsilon^7 + 0.112215129 a^{9\alpha}\varepsilon^8 + 0.03384213214 a^{10\alpha}\varepsilon^9 \\
&\quad + 0.009167879378 a^{11\alpha}\varepsilon^{10} + 0.001927981749 a^{12\alpha}\varepsilon^{11} \\
&\quad + 0.0002525543343 a^{13\alpha}\varepsilon^{12}
\end{aligned} \tag{30}
$$

$$
\begin{aligned}
A_2 &= -4.0 - 10.6666667 a^{\alpha}\varepsilon - 15.2 a^{2\alpha}\varepsilon^2 - 15.81375661 a^{3\alpha}\varepsilon^3 \\
&\quad - 13.42081129 a^{4\alpha}\varepsilon^4 - 8.763597884 a^{5\alpha}\varepsilon^5 - 4.984650598 a^{6\alpha}\varepsilon^6 \\
&\quad - 2.434521467 a^{7\alpha}\varepsilon^7 - 1.009936161 a^{8\alpha}\varepsilon^8 - 0.3384213214 a^{9\alpha}\varepsilon^9 \\
&\quad - 0.1008466732 a^{10\alpha}\varepsilon^{10} - 0.02313578099 a^{11\alpha}\varepsilon^{11} \\
&\quad - 0.003283206347 a^{12\alpha}\varepsilon^{12}
\end{aligned} \tag{31}
$$

$$
\begin{aligned}
A_3 &= 5.333333333\varepsilon + 15.2 a^{\alpha}\varepsilon^2 + 23.72063492 a^{2\alpha}\varepsilon^3 + 26.84162257 a^{3\alpha}\varepsilon^4 \\
&\quad + 21.90899471 a^{4\alpha}\varepsilon^5 + 14.95395179 a^{5\alpha}\varepsilon^6 + 8.520825136 a^{6\alpha}\varepsilon^7 \\
&\quad + 4.039744643 a^{7\alpha}\varepsilon^8 + 1.522895946 a^{8\alpha}\varepsilon^9 + 0.5042333658 a^{9\alpha}\varepsilon^{10} \\
&\quad + 0.1272467954 a^{10\alpha}\varepsilon^{11} + 0.01969923808 a^{11\alpha}\varepsilon^{12}
\end{aligned} \tag{32}
$$

$$A_4 = -5.06666667\varepsilon^2 - 15.81375661a^\alpha\varepsilon^3 - 26.84162257a^{2\alpha}\varepsilon^4$$
$$- 29.21199295a^{3\alpha}\varepsilon^5 - 24.92325299a^{4\alpha}\varepsilon^6 - 17.04165027a^{5\alpha}\varepsilon^7$$
$$- 9.426070834a^{6\alpha}\varepsilon^8 - 4.061055857a^{7\alpha}\varepsilon^9 - 1.512700097a^{8\alpha}\varepsilon^{10}$$
$$- 0.4241559847a^{9\alpha}\varepsilon^{11} - 0.07223053962a^{10\alpha}\varepsilon^{12}$$
(33)

$$A_5 = 3.953439153\varepsilon^3 + 13.42081129a^\alpha\varepsilon^4 + 21.90899471a^{2\alpha}\varepsilon^5$$
$$+ 24.92325299a^{3\alpha}\varepsilon^6 + 21.30206284a^{4\alpha}\varepsilon^7 + 14.13910625a^{5\alpha}\varepsilon^8$$
$$+ 7.106847749a^{6\alpha}\varepsilon^9 + 3.025400195a^{7\alpha}\varepsilon^{10} + 0.954350657a^{8\alpha}\varepsilon^{11}$$
$$+ 0.1805763491a^{9\alpha}\varepsilon^{12}$$
(34)

$$A_6 = -2.684162257\varepsilon^4 - 8.763597884a^\alpha\varepsilon^5 - 14.95395179a^{2\alpha}\varepsilon^6$$
$$- 17.04165027a^{3\alpha}\varepsilon^7 - 14.13910625a^{4\alpha}\varepsilon^8 - 8.528217299a^{5\alpha}\varepsilon^9$$
$$- 4.235560273a^{6\alpha}\varepsilon^{10} - 1.526961545a^{7\alpha}\varepsilon^{11} - 0.3250374283a^{8\alpha}\varepsilon^{12}$$
(35)

$$A_7 = 1.460599647\varepsilon^5 + 4.984650598a^\alpha\varepsilon^6 + 8.520825136a^{2\alpha}\varepsilon^7$$
$$+ 9.426070834a^{3\alpha}\varepsilon^8 + 7.106847749a^{4\alpha}\varepsilon^9 + 4.235560273a^{5\alpha}\varepsilon^{10}$$
$$+ 1.781455136a^{6\alpha}\varepsilon^{11} + 0.4333832377a^{7\alpha}\varepsilon^{12}$$
(36)

$$A_8 = -0.7120929425\varepsilon^6 - 2.434521467a^\alpha\varepsilon^7 - 4.039744643a^{2\alpha}\varepsilon^8$$
$$- 4.061055857a^{3\alpha}\varepsilon^9 - 3.025400195a^{4\alpha}\varepsilon^{10} - 1.526961545a^{5\alpha}\varepsilon^{11}$$
$$- 0.4333832377a^{6\alpha}\varepsilon^{12}$$
(37)

$$A_9 = 0.3043151834\varepsilon^7 + 1.009936161a^\alpha\varepsilon^8 + 1.522895946a^{2\alpha}\varepsilon^9$$
$$+ 1.512700097a^{3\alpha}\varepsilon^{10} + 0.9543509657a^{4\alpha}\varepsilon^{11} + 0.3250374283a^{5\alpha}\varepsilon^{12}$$
(38)

$$A_{10} = -0.112215129\varepsilon^8 - 0.3384213214a^\alpha\varepsilon^9 - 0.5042333658a^{2\alpha}\varepsilon^{10}$$
$$- 0.4241559847a^{3\alpha}\varepsilon^{11} - 0.1805753491a^{4\alpha}\varepsilon^{12}$$
(39)

$$A_{11} = 0.03384213214\varepsilon^9 + 0.1008466732a^\alpha\varepsilon^{10} + 0.1272467954a^{2\alpha}\varepsilon^{11}$$
$$+ 0.07223053962a^{3\alpha}\varepsilon^{12}$$
(40)

$$A_{12} = -0.009167879378\varepsilon^{10} - 0.02313578099a^\alpha\varepsilon^{11} - 0.01969923808a^{2\alpha}\varepsilon^{12}$$
(41)

$$A_{13} = 0.001927981749\varepsilon^{11} + 0.003283206347a^\alpha\varepsilon^{12}$$
(42)

$$A_{14} = 0.0002525543343\varepsilon^{12}$$
(43)

$$B(r) = P(v)\left\{ -\alpha(3P(v) - 2P(v)v + 1)r^{\alpha} + (a^{\alpha} - r^{\alpha})(P(v) + 1)^2 \right\}$$
$$= B_1 + B_2 r^{\alpha} + B_3 r^{2\alpha} + B_4 r^{3\alpha} + B_5 r^{4\alpha} + B_6 r^{5\alpha} + B_7 r^{6\alpha} + B_8 r^{7\alpha} \tag{44}$$
$$+ B_9 r^{8\alpha} + B_{10} r^{9\alpha} + B_{11} r^{10\alpha} + B_{12} r^{11\alpha} + B_{13} r^{12\alpha} + B_{14} r^{13\alpha}$$

$$
\begin{aligned}
B_1 = {}& 4a^{\alpha} + +5.333333333a^{2\alpha}\varepsilon + 5.066666667a^{3\alpha}\varepsilon^2 \\
& + 3.953439153a^{4\alpha}\varepsilon^3 + 2.684162257a^{5\alpha}\varepsilon^4 + 1.460599647a^{6\alpha}\varepsilon^5 \\
& + 0.7120929425a^{7\alpha}\varepsilon^6 + 0.304315834a^{8\alpha}\varepsilon^7 + 0.112215129a^{9\alpha}\varepsilon^8 \\
& + 0.03384213214a^{10\alpha}\varepsilon^9 + 0.009167879378a^{11\alpha}\varepsilon^{10} + 0.001927981749a^{12\alpha}\varepsilon^{11} \\
& + 0.0002525543343a^{13\alpha}\varepsilon^{12}
\end{aligned}
\tag{45}
$$

$$
\begin{aligned}
B_2 = {}& -4.0 - 4\alpha - 10.66666667a^{\alpha}\varepsilon - 2.666666667a^{\alpha}\alpha\varepsilon \\
& -15.22222222a^{2\alpha}\varepsilon^2 - 1.155555556a^{2\alpha}\alpha\varepsilon^2 - 15.81375661a^{3\alpha}\varepsilon^3 \\
& -0.237037037a^{3\alpha}\alpha\varepsilon^3 - 13.42081129a^{4\alpha}\varepsilon^4 + 0.1264197531a^{4\alpha}\alpha\varepsilon^4 \\
& -8.763597884a^{5\alpha}\varepsilon^5 + 0.3386243386a^{5\alpha}\alpha\varepsilon^5 - 4.984650598a^{6\alpha}\varepsilon^6 \\
& +0.184856639a^{6\alpha}\alpha\varepsilon^6 - 2.434521467a^{7\alpha}\varepsilon^7 + 0.08063917583a^{7\alpha}\alpha\varepsilon^7 \\
& -1.009936161a^{8\alpha}\varepsilon^8 + 0.02868189954a^{8\alpha}\alpha\varepsilon^8 - 0.3384213214a^{9\alpha}\varepsilon^9 \\
& +0.007990976985a^{9\alpha}\alpha\varepsilon^9 - 0.1008466732a^{10\alpha}\varepsilon^{10} - 0.02313578099a^{11\alpha}\varepsilon^{11} \\
& -0.003283206347a^{12\alpha}\varepsilon^{12}
\end{aligned}
\tag{46}
$$

$$
\begin{aligned}
B_3 = {}& 5.333333333\varepsilon + 2.666666667a\varepsilon + 15.2a^{\alpha}\varepsilon^2 \\
& + 2.311111111a^{\alpha}\alpha\varepsilon^2 + 23.72063492a^{2\alpha}\varepsilon^3 + 0.711111111a^{2\alpha}\alpha\varepsilon^3 \\
& + 26.84162257a^{3\alpha}\varepsilon^4 - 0.5056790123a^{3\alpha}\alpha\varepsilon^4 + 21.90899471a^{4\alpha}\varepsilon^5 \\
& - 1.693121693a^{4\alpha}\alpha\varepsilon^5 + 14.95395179a^{5\alpha}\varepsilon^6 - 1.109139834a^{5\alpha}\alpha\varepsilon^6 \\
& + 8.520825136a^{6\alpha}\varepsilon^7 - 0.5644742308a^{6\alpha}\alpha\varepsilon^7 + 4.039744643a^{7\alpha}\varepsilon^8 \\
& - 0.2294551963a^{7\alpha}\alpha\varepsilon^8 + 1.522895946a^{8\alpha}\varepsilon^9 - 0.07191879287a^{8\alpha}\alpha\varepsilon^9 \\
& + 0.5042333658a^{9\alpha}\varepsilon^{10} + 0.1272467954a^{10\alpha}\varepsilon^{11} + 0.01969923808a^{11\alpha}\varepsilon^{12}
\end{aligned}
\tag{47}
$$

$$B_4 = -5.066666667\varepsilon^2 - 1.155555556\alpha\varepsilon^2 - 15.81375661a^\alpha\varepsilon^3$$
$$- 0.711111111a^\alpha\alpha\varepsilon^3 - 26.84162257a^{2\alpha}\varepsilon^4 + 0.7585185185a^{2\alpha}\alpha\varepsilon^4$$
$$- 29.21199295a^{3\alpha}\varepsilon^5 + 3.386243386a^{3\alpha}\alpha\varepsilon^5 - 24.92325299a^{4\alpha}\varepsilon^6$$
$$+ 2.772849584a^{4\alpha}\alpha\varepsilon^6 - 17.04165027a^{5\alpha}\varepsilon^7 + 1.693422693a^{5\alpha}\alpha\varepsilon^7$$
$$- 9.426070834a^{6\alpha}\varepsilon^8 + 0.803093187a^{6\alpha}\alpha\varepsilon^8 - 4.061055857a^{7\alpha}\varepsilon^9$$
$$+ 0.2876751715a^{7\alpha}\alpha\varepsilon^9 - 1.512700097a^{8\alpha}\varepsilon^{10} - 0.4241559847a^{9\alpha}\varepsilon^{11}$$
$$- 0.07223053962a^{10\alpha}\varepsilon^{12}$$

(48)

$$B_5 = 3.953439153\varepsilon^3 + 0.237037037\alpha\varepsilon^3 + 13.420881129a^\alpha\varepsilon^4$$
$$- 0.5056790123a^\alpha\alpha\varepsilon^4 + 21.90899471a^{2\alpha}\varepsilon^5 - 3.386243386a^{2\alpha}\alpha\varepsilon^5$$
$$+ 24.92325299a^{3\alpha}\varepsilon^6 - 3.697132779a^{3\alpha}\alpha\varepsilon^6 + 21.30206284a^{4\alpha}\varepsilon^7$$
$$- 2.822371154a^{4\alpha}\alpha\varepsilon^7 + 14.13910625a^{5\alpha}\varepsilon^8 - 1.606186374a^{5\alpha}\alpha\varepsilon^8$$
$$+ 7.106847749a^{6\alpha}\varepsilon^9 - 0.6712420668a^{6\alpha}\alpha\varepsilon^9 + 3.025400195a^{7\alpha}\varepsilon^{10}$$
$$+ 0.9543509657a^{8\alpha}\varepsilon^{11} + 0.1805763491a^{9\alpha}\varepsilon^{12}$$

(49)

$$B_6 = -2.684162257\varepsilon^4 + 0.1264197531\alpha\varepsilon^4 - 8.763597884a^\alpha\varepsilon^5$$
$$+ 1.693121693a^\alpha\alpha\varepsilon^5 - 14.95395179a^{2\alpha}\varepsilon^6 + 2.772849584a^{2\alpha}\alpha\varepsilon^6$$
$$- 17.04165027a^{3\alpha}\varepsilon^7 + 2.822371154a^{3\alpha}\alpha\varepsilon^7 - 14.13910625a^{4\alpha}\varepsilon^8$$
$$+ 2.007732968a^{4\alpha}\alpha\varepsilon^8 - 8.528217299a^{5\alpha}\varepsilon^9 + 1.0068631a^{5\alpha}\alpha\varepsilon^9$$
$$- 4.235560273a^{6\alpha}\varepsilon^{10} - 1.526961545a^{7\alpha}\varepsilon^{11} - 0.325037428a^{8\alpha}\varepsilon^{12}$$

(50)

$$B_7 = 1.460599647\varepsilon^5 - 0.3386243386\alpha\varepsilon^5 + 4.984650598a^\alpha\varepsilon^6$$
$$- 1.109139834a^\alpha\alpha\varepsilon^6 + 8.520825136a^{2\alpha}\varepsilon^7 - 1.693422693a^{2\alpha}\alpha\varepsilon^7$$
$$+ 9.426070834a^{3\alpha}\varepsilon^8 - 1.606186374a^{3\alpha}\alpha\varepsilon^8 + 7.106847749a^{4\alpha}\varepsilon^9$$
$$- 1.0068631a^{4\alpha}\alpha\varepsilon^9 + 4.235560272a^{5\alpha}\varepsilon^{10} + 1.781455136a^{6\alpha}\varepsilon^{11}$$
$$+ 0.4333832377a^{7\alpha}\varepsilon^{12}$$

(51)

$$B_8 = -0.7120929425\varepsilon^6 + 0.184856639\alpha\varepsilon^6 - 2.434521467a^\alpha\varepsilon^7$$
$$+ 0.5644742308a^\alpha\alpha\varepsilon^7 - 4.039744743a^{2\alpha}\varepsilon^8 + 0.803093187a^{2\alpha}\alpha\varepsilon^8$$
$$- 4.061055857a^{3\alpha}\varepsilon^9 + 0.6712420668a^{3\alpha}\alpha\varepsilon^9 - 3.025400195a^{4\alpha}\varepsilon^{10}$$
$$- 1.526961545a^{5\alpha}\varepsilon^{11} - 0.4333832377a^{6\alpha}\varepsilon^{12}$$

(52)

$$B_9 = 0.3043151834\varepsilon^7 - 0.08063917583\alpha\varepsilon^7 + 1.009936161a^\alpha\varepsilon^8$$
$$- 0.2294551963a^\alpha\alpha\varepsilon^8 + 1.522895946a^{2\alpha}\varepsilon^9 - 0.2876751715a^{2\alpha}\alpha\varepsilon^9 \qquad (53)$$
$$+ 1.512700097a^{3\alpha}\varepsilon^{10} + 0.9543509657a^{4\alpha}\varepsilon^{11} + 0.3250374283a^{5\alpha}\varepsilon^{12}$$

$$B_{10} = -0.112215129\varepsilon^8 + 0.02868189954\alpha\varepsilon^8 - 0.3384213214a^\alpha\varepsilon^9$$
$$+ 0.07191879287a^\alpha\alpha\varepsilon^9 - 0.5042333658a^{2\alpha}\varepsilon^{10} - 0.4241559847a^{3\alpha}\varepsilon^{11} \qquad (54)$$
$$- 0.1805763491a^{4\alpha}\varepsilon^{12}$$

$$B_{11} = 0.03384213214\varepsilon^9 - 0.007990976985\alpha\varepsilon^9 + 0.1008466732a^\alpha\varepsilon^{10}$$
$$+ 0.1272467954a^{2\alpha}\varepsilon^{11} + 0.07223053962a^{3\alpha}\varepsilon^{12} \qquad (55)$$

$$B_{12} = -0.009167879378\varepsilon^{10} - 0.02313578098a^\alpha\varepsilon^{11} - 0.01969923808a^{2\alpha}\varepsilon^{12} \qquad (56)$$

$$B_{13} = 0.001927981749\varepsilon^{11} + 0.003283206347a^\alpha\varepsilon^{12} \qquad (57)$$

$$B_{14} = 0.0002525543343\varepsilon^{12} \qquad (58)$$

$$C(r) = \frac{\sigma^2 a^\alpha}{gh_0}[P(\nu)\nu + 1][P(\nu) + 1]^2 r^2$$
$$= C_0(C_1 r^2 + C_2 r^{2+\alpha} + C_3 r^{2+2\alpha} + C_4 r^{2+3\alpha} + C_5 r^{2+4\alpha} + C_6 r^{2+5\alpha} + C_7 r^{2+6\alpha} + C_8 r^{2+7\alpha} \qquad (59)$$
$$+ C_9 r^{2+8\alpha} + C_{10} r^{2+9\alpha} + C_{11} r^{2+10\alpha} + C_{12} r^{2+11\alpha} + C_{13} r^{2+12\alpha} + C_{14} r^{2+13\alpha})$$

$$C_0 = \frac{\sigma^2 a^\alpha}{gh_0} \qquad (60)$$

$$C_1 = 4.0 + 6.666666667a^\alpha\varepsilon + 7.199999999a^{2\alpha}\varepsilon^2$$
$$+ 6.184126984a^{3\alpha}\varepsilon^3 + 4.547160494a^{4\alpha}\varepsilon^4 + 2.882821869a^{5\alpha}\varepsilon^5$$
$$+ 1.531420509a^{6\alpha}\varepsilon^6 + 0.732427125a^{7\alpha}\varepsilon^7 + 0.3083106719a^{8\alpha}\varepsilon^8 \qquad (61)$$
$$+ 0.112215129a^{9\alpha}\varepsilon^9 + 0.03384213214a^{10\alpha}\varepsilon^{10} + 0.009167879378a^{11\alpha}\varepsilon^{11}$$
$$+ 0.001927981749a^{12\alpha}\varepsilon^{12} + 0.0002525543343a^{13\alpha}\varepsilon^{13}$$

$$C_2 = -6.666666667\varepsilon - 14.4a^\alpha\varepsilon^2 - 18.55238095a^{2\alpha}\varepsilon^3$$
$$- 18.18864198a^{3\alpha}\varepsilon^4 - 14.41410935a^{4\alpha}\varepsilon^5 - 9.188523054a^{5\alpha}\varepsilon^6$$
$$- 5.126989875a^{6\alpha}\varepsilon^7 - 2.466485375a^{7\alpha}\varepsilon^8 - 1.009936161a^{8\alpha}\varepsilon^9 \qquad (62)$$
$$- 0.3384213214a^{9\alpha}\varepsilon^{10} - 0.1008466732a^{10\alpha}\varepsilon^{11} - 0.02313578099a^{11\alpha}\varepsilon^{12}$$
$$- 0.003283206347a^{12\alpha}\varepsilon^{13}$$

17

$$C_3 = 7.199999999\varepsilon^2 + 18.55238095a^\alpha\varepsilon^3 + 27.28296296a^{2\alpha}\varepsilon^4$$
$$+ 28.82821869a^{3\alpha}\varepsilon^5 + 22.97130763a^{4\alpha}\varepsilon^6 + 15.38096963a^{5\alpha}\varepsilon^7$$
$$+ 8.632698813a^{6\alpha}\varepsilon^8 + 4.039744643a^{7\alpha}\varepsilon^9 + 1.522895946a^{8\alpha}\varepsilon^{10}$$
$$+ 0.5042333658a^{9\alpha}\varepsilon^{11} + 0.1272467954a^{10\alpha}\varepsilon^{12} + 0.01969923808a^{11\alpha}\varepsilon^{13}$$

(63)

$$C_4 = -6.184126984\varepsilon^3 - 18.18864198a^\alpha\varepsilon^4 - 28.82821869a^{2\alpha}\varepsilon^5$$
$$- 30.62841018a^{3\alpha}\varepsilon^6 - 25.63494938a^{4\alpha}\varepsilon^7 - 17.26539763a^{5\alpha}\varepsilon^8$$
$$- 9.426070834a^{6\alpha}\varepsilon^9 - 4.061055857a^{7\alpha}\varepsilon^{10} - 1.512700097a^{8\alpha}\varepsilon^{11}$$
$$- 0.4241559847a^{9\alpha}\varepsilon^{12} - 0.07223053962a^{10\alpha}\varepsilon^{13}$$

(64)

$$C_5 = 4.547160494\varepsilon^4 + 14.41410935a^\alpha\varepsilon^5 + 22.97130763a^{2\alpha}\varepsilon^6$$
$$+ 25.63494938a^{3\alpha}\varepsilon^7 + 21.58174703a^{4\alpha}\varepsilon^8 + 14.13910625a^{5\alpha}\varepsilon^9$$
$$+ 7.106847749a^{6\alpha}\varepsilon^{10} + 3.025400195a^{7\alpha}\varepsilon^{11} + 0.9543409657a^{8\alpha}\varepsilon^{12}$$
$$+ 0.1805763491a^{9\alpha}\varepsilon^{13}$$

(65)

$$C_6 = -2.882821869\varepsilon^5 - 9.188523054a^\alpha\varepsilon^6 - 15.38096963a^{2\alpha}\varepsilon^7$$
$$- 17.26539763a^{3\alpha}\varepsilon^8 - 14.13910625a^{4\alpha}\varepsilon^9 - 8.528217299a^{5\alpha}\varepsilon^{10}$$
$$- 4.235560273a^{6\alpha}\varepsilon^{11} - 1.526961545a^{7\alpha}\varepsilon^{12} - 0.3250374283a^{8\alpha}\varepsilon^{13}$$

(66)

$$C_7 = 1.531420509\varepsilon^6 + 5.126989875a^\alpha\varepsilon^7 + 8.632698813a^{2\alpha}\varepsilon^8$$
$$+ 9.426070834a^{3\alpha}\varepsilon^9 + 7.106847749a^{4\alpha}\varepsilon^{10} + 4.235560273a^{5\alpha}\varepsilon^{11}$$
$$+ 1.781455136a^{6\alpha}\varepsilon^{12} + 0.4333832377a^{7\alpha}\varepsilon^{13}$$

(67)

$$C_8 = -0.732427125\varepsilon^7 - 2.466485375a^\alpha\varepsilon^8 - 4.039744643a^{2\alpha}\varepsilon^9$$
$$- 4.061055857a^{3\alpha}\varepsilon^{10} - 3.025400195a^{4\alpha}\varepsilon^{11} - 1.526961545a^{5\alpha}\varepsilon^{12}$$
$$- 0.4333832377a^{6\alpha}\varepsilon^{13}$$

(68)

$$C_9 = 0.3083106719\varepsilon^8 + 1.009936161a^\alpha\varepsilon^9 + 1.522895946a^{2\alpha}\varepsilon^{10}$$
$$+ 1.512700097a^{3\alpha}\varepsilon^{11} + 0.9543509657a^{4\alpha}\varepsilon^{12} + 0.3250374283a^{5\alpha}\varepsilon^{13}$$

(69)

$$C_{10} = -0.112215129\varepsilon^9 - 0.3384213214a^\alpha\varepsilon^{10} - 0.5042333658a^{2\alpha}\varepsilon^{11}$$
$$- 0.4241559847a^{3\alpha}\varepsilon^{12} - 0.1805763491a^{4\alpha}\varepsilon^{13}$$

(70)

$$C_{11} = 0.03384213214\varepsilon^{10} + 0.1008466732a^\alpha\varepsilon^{11} + 0.1272467954a^{2\alpha}\varepsilon^{12}$$
$$+ 0.07223053962a^{3\alpha}\varepsilon^{13}$$

(71)

$$C_{12} = -0.009167879378\varepsilon^{11} - 0.02313578099a^{\alpha}\varepsilon^{12} - 0.01969923808a^{2\alpha}\varepsilon^{13} \tag{72}$$

$$C_{13} = 0.001927981749\varepsilon^{12} + 0.003283206347a^{\alpha}\varepsilon^{13} \tag{73}$$

$$C_{14} = 0.0002525543343\varepsilon^{13} \tag{74}$$

$$D(r) = P(v)(a^{\alpha} - r^{\alpha})[P(v) + 1]^2 = A(r) \tag{75}$$

Appendix B. Recurrence relations for $a_{m,n}$

For $\alpha = 1$,

$$a_{0,n} = \text{arbitrary value} \tag{76}$$

$$a_{m,n} = -\frac{[A_2(m+n-1)(m+n-2) + B_2(m+n) - n^2D_2]a_{m-1,n}}{A_1(m+n)(m+n-1) + B_1(m+n) - n^2D_1} \qquad m = 1 \tag{77}$$

$$a_{m,n} = -\frac{\sum_{j=2}^{l}[A_j(m+n-j+1)(m+n-j) + B_j(m+n-j+1) - n^2D_j]a_{m-j+1}}{A_1(m+n)(m+n-1) + B_1(m+n) - n^2D_1}$$
$$-\frac{\sum_{j=2}^{l-1}C_0C_{j-1}a_{m-j}}{A_1(m+n)(m+n-1) + B_1(m+n) - n^2D_1}$$
$$m = l-1 \quad \text{where} \quad l = 3, \ 4, \ \cdots, \ 14 \tag{78}$$

$$a_{m,n} = -\frac{\sum_{j=2}^{14}[A_j(m+n-j+1)(m+n-j) + B_j(m+n-j+1) - n^2D_j]a_{m-j+1}}{A_1(m+n)(m+n-1) + B_1(m+n) - n^2D_1}$$
$$-\frac{\sum_{j=2}^{14}C_0C_{j-1}a_{m-j}}{A_1(m+n)(m+n-1) + B_1(m+n) - n^2D_1}$$
$$m = 14 \tag{79}$$

$$a_{m,n} = -\frac{\sum_{j=2}^{14}[A_j(m+n-j+1)(m+n-j)+B_j(m+n-j+1)-n^2D_j]a_{m-j+1}}{A_1(m+n)(m+n-1)+B_1(m+n)-n^2D_1}$$

$$-\frac{\sum_{j=2}^{15}C_0C_{j-1}a_{m-j}}{A_1(m+n)(m+n-1)+B_1(m+n)-n^2D_1}$$

$$m \geq 15 \qquad (80)$$

For $\alpha = 2$,

$$a_{0,n} = \text{arbitrary value} \qquad (81)$$

$$a_{m,n} = 0 \qquad\qquad m = 1 \qquad (82)$$

$$a_{m,n} = -\frac{\sum_{j=2}^{l}[A_j(m+n-2(j-1))(m+n-2(j-1)-1)+B_j(m+n-2(j-1))]a_{m-2(j-1)}}{A_1(m+n)(m+n-1)+B_1(m+n)-n^2D_1}$$

$$-\frac{\sum_{j=2}^{l}(C_0C_{j-1}-n^2D_j)a_{m-2(j-1)}}{A_1(m+n)(m+n-1)+B_1(m+n)-n^2D_1}$$

$$2(l-1) \leq m < 2l \quad \text{where} \quad l = 2,\ 3,\ \cdots,\ 14 \qquad (83)$$

$$a_{m,n} = -\frac{\sum_{j=2}^{14}[A_j(m+n-2(j-1))(m+n-2(j-1)-1)+B_j(m+n-2(j-1))]a_{m-2(j-1)}}{A_1(m+n)(m+n-1)+B_1(m+n)-n^2D_1}$$

$$-\frac{\sum_{j=2}^{15}(C_0C_{j-1}-n^2D_j)a_{m-2(j-1)}}{A_1(m+n)(m+n-1)+B_1(m+n)-n^2D_1}$$

$$m \geq 28 \qquad (84)$$

For $\alpha \geq 3$,

$$a_{0,n} = \text{arbitrary value} \tag{85}$$

$$a_{m,n} = 0 \qquad\qquad m = 1 \tag{86}$$

$$a_{m,n} = -\frac{\displaystyle\sum_{j=1}^{1} C_0 C_j a_{m-(j-1)\alpha-2,n}}{A_1(m+n)(m+n-1) + B_1(m+n) - n^2 D_1} \qquad 2 \le m < \alpha \tag{87}$$

$$a_{m,n} = -\frac{\displaystyle\sum_{j=1}^{l} C_0 C_j a_{m-(j-1)\alpha-2,n}}{A_1(m+n)(m+n-1) + B_1(m+n) - n^2 D_1}$$

$$-\frac{\displaystyle\sum_{j=1}^{l} [A_{j+1}(m+n-j\alpha)(m+n-j\alpha-1) + B_{j+1}(m+n-j\alpha) - n^2 D_{j+1}] a_{m-j\alpha,n}}{A_1(m+n)(m+n-1) + B_1(m+n) - n^2 D_1}$$

$$l\alpha \le m < l\alpha + 2 \quad \text{where} \quad l = 1,\ 2,\ \cdots,\ 13 \tag{88}$$

$$a_{m,n} = -\frac{\displaystyle\sum_{j=1}^{l+1} C_0 C_j a_{m-(j-1)\alpha-2,n}}{A_1(m+n)(m+n-1) + B_1(m+n) - n^2 D_1}$$

$$-\frac{\displaystyle\sum_{j=1}^{l} [A_{j+1}(m+n-j\alpha)(m+n-j\alpha-1) + B_{j+1}(m+n-j\alpha) - n^2 D_{j+1}] a_{m-j\alpha,n}}{A_1(m+n)(m+n-1) + B_1(m+n) - n^2 D_1}$$

$$l\alpha + 2 \le m < (l+1)\alpha \quad \text{where} \quad l = 1,\ 2,\ \cdots,\ 12 \tag{89}$$

$$a_{m,n} = -\frac{\displaystyle\sum_{j=1}^{14} C_0 C_j \beta_{m-(j-1)\alpha-2,n}}{A_1(m+n)(m+n-1) + B_1(m+n) - n^2 D_1}$$

$$-\frac{\displaystyle\sum_{j=1}^{13} [A_{j+1}(m+n-j\alpha)(m+n-j\alpha-1) + B_{j+1}(m+n-j\alpha) - n^2 D_{j+1}] a_{m-j\alpha,n}}{A_1(m+n)(m+n-1) + B_1(m+n) - n^2 D_1}$$

$$m \ge 13\alpha + 2 \tag{90}$$

References

Berkhoff, J.C.W., 1972. Computation of combined refraction-diffraction. Proc. 13th Coastal Eng. Conf., ASCE, pp. 471-490.

Copeland, G.J.M., 1985. A practical alternative to the mild-slope wave equation. Coastal Engineering 9, 125-149.

Homma, S., 1950. On the behavior of seismic sea waves around circular island. Geophys. Mag. XXI, 199-208.

Hunt, J.N., 1979. Direct solution of wave dispersion equation. J. Waterw., Port, Coast., Ocean Div. Proc. ASCE 105, 457-459.

Jonsson, I.G., Skovgaard, O., Brink-Kjaer, O., 1976. Diffraction and refraction calculations for waves incident on an island. J. Mar. Res. 34, 469-496.

Liu, H.-W., Lin, P., Shankar, N. J., 2004. An analytical solution of the mild-slope equation for waves around a circular island on a paraboloidal shoal. Coastal Engineering 51, 421-437.

Liu, P.L.-F., 1986. Effects of depth discontinuity on harbor oscillations. Coastal Engineering 10, 395-404.

Longuet-Higgins, M.S., 1967. On the trapping of wave energy round islands. J. Fluid Mech. 29, 781-821.

Press, W.H., Teukolsky, S.A., Vetterling, W.T., Flannery, B.P., 1992. Numerical Recipes in FORTRAN: The Art of Scientific Computing, Cambridge Univ. Press, Cambridge.

Suh, K.-D., Jung, T.-H., Haller, M.C., 2005. Long waves propagating over a circular bowl pit. Wave Motion 42, 143-154.

Suh, K.D., Lee, C., Park, Y.-H., Lee, T.H., 2001. Experimental verification of horizontal two-dimensional modified mild-slope equation model. Coastal Engineering 44, 1-12.

Vastano, A.C., Reid, R.O., 1967. Tsunami response for island: verification of a numerical procedure. J. Mar. Res. 25, 129-139.

Yu, X., Zhang, B., 2003. An extended analytic solution for combined refraction and diffraction of long waves over circular shoals. Ocean Engineering 30, 1253-1267.

Zhu, S., Zhang, Y., 1996. Scattering of long waves around a circular island mounted on a conical shoal. Wave Motion 23, 353-362.
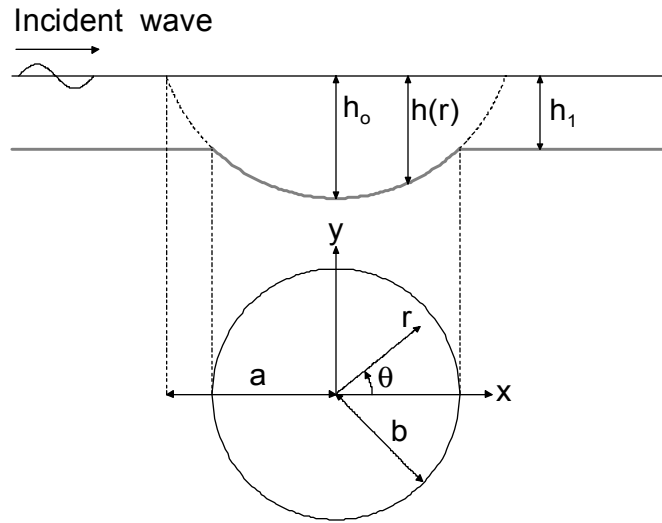
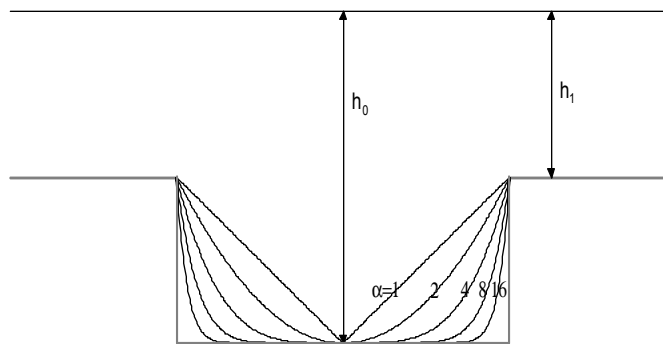Fig. 1. Definition sketch of an axi-symmetric pit located in an otherwise constant depth region.

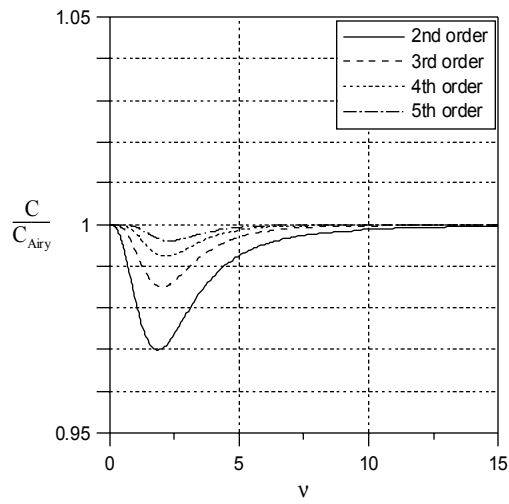Fig. 2. Cross-sectional views along the x-axis of axi-symmetric pits of various values of α.

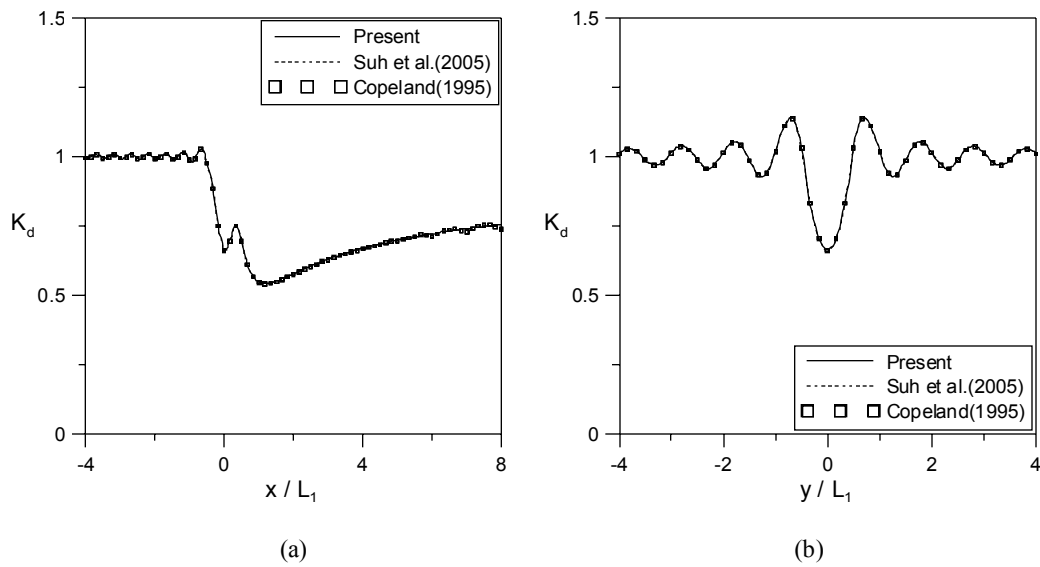Fig. 3. Comparison of normalized phase speeds for different orders of Hunt's solution.

(a)

(b)

Fig. 4. Comparison among analytic and numerical solutions for diffraction coefficients for an axi-symmetric pit with $h_1 = 3.2$ m, $h_0 = 6.4$ m, $b = 0.5L_1$, $k_1h_1 = 0.083$, $k_0h_0 = 0.118$, and $\alpha = 2$: along (a) x-axis; (b) y-axis.

(a)   (b)
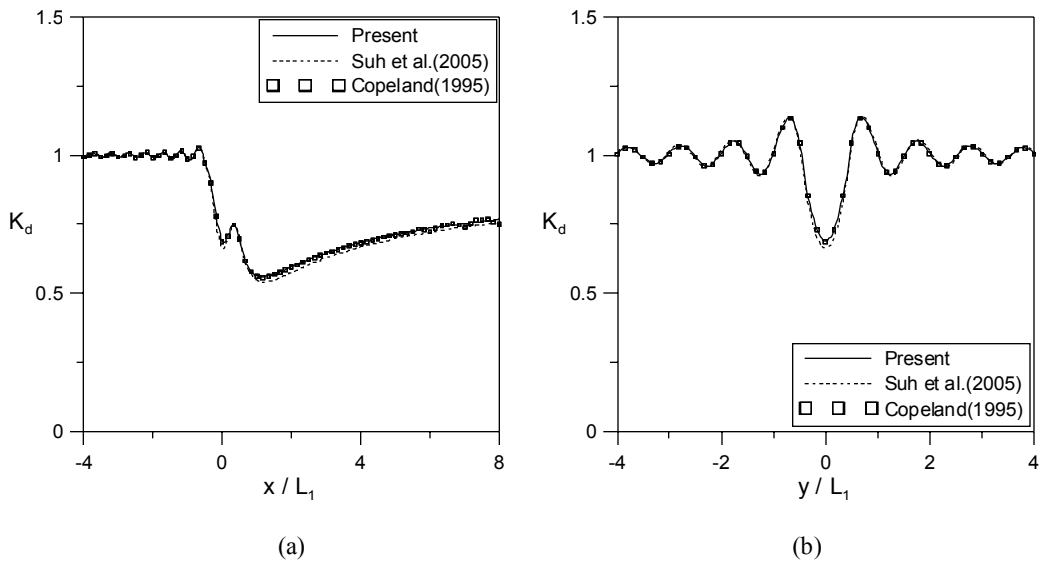
Fig. 5. Same as Fig. 4 except for $k_1 h_1 = 0.334$ and $k_0 h_0 = 0.481$.

(a)   (b)
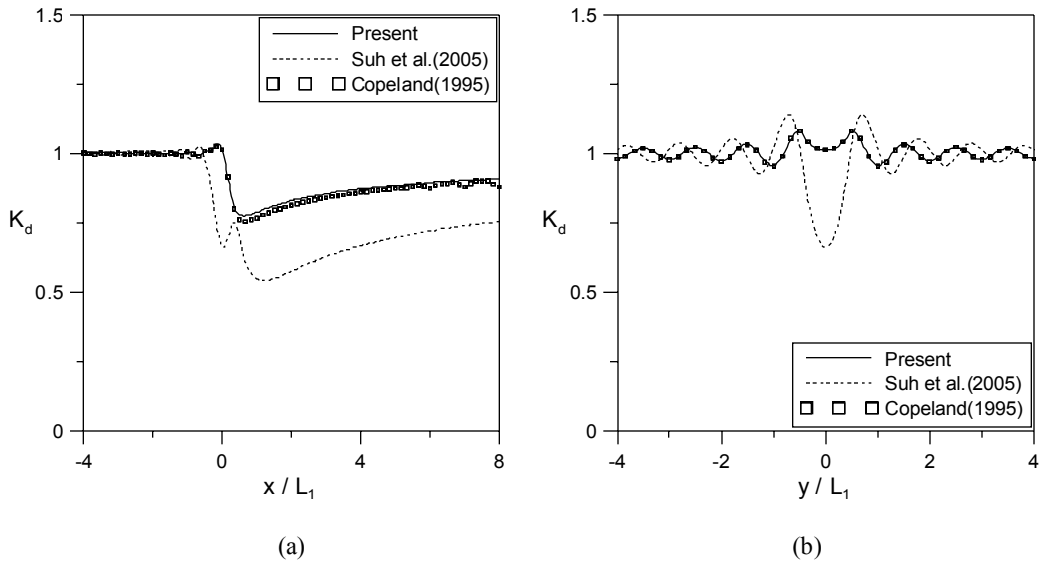
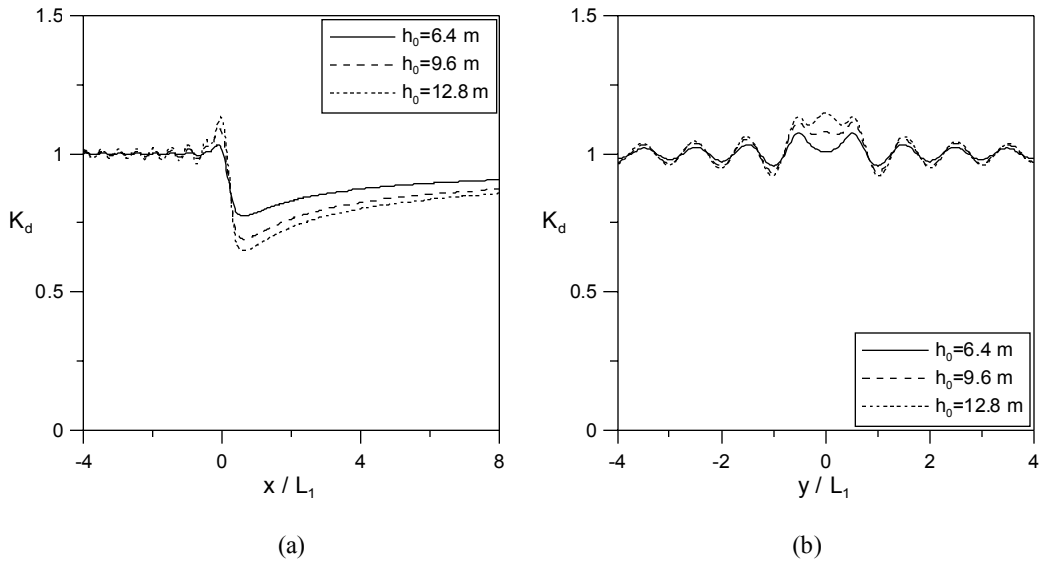Fig. 6. Same as Fig. 4 except for $k_1 h_1 = 1.336$ and $k_0 h_0 = 2.368$.

(a)   (b)
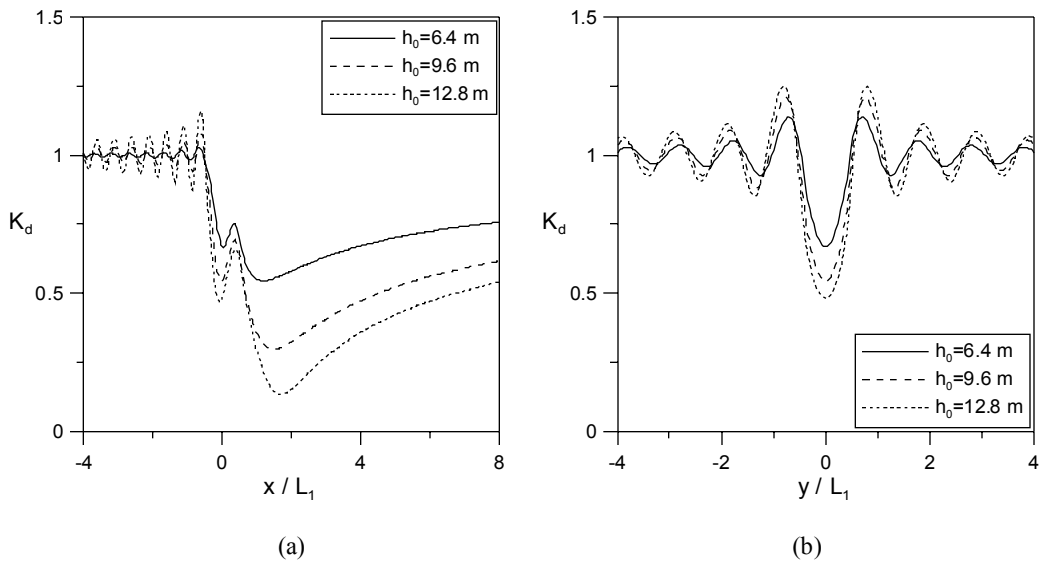
Fig. 7. Comparison of diffraction coefficients among pits with different central depths but with the same radius and $h_1 = 3.2$ m, $b = 0.5L_1$, $k_1 h_1 = 0.167$, and $\alpha = 2$: along (a) x-axis; (b) y-axis.

(a)   (b)
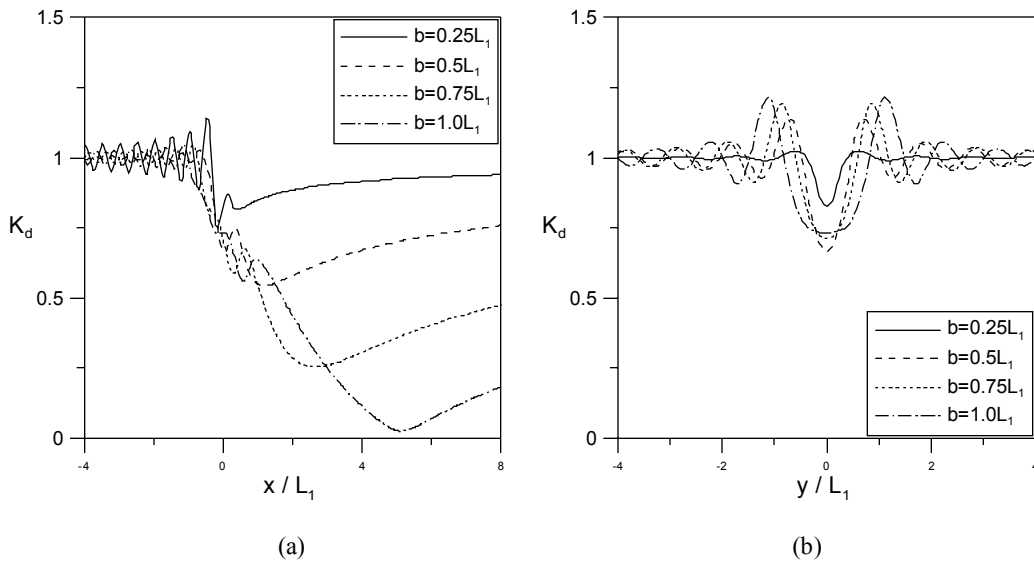
Fig. 8. Same as Fig. 7 except for $k_1 h_1 = 1.336$.

(a)   (b)

Fig. 9. Comparison of diffraction coefficients among pits with different radii but with the same central depth and $h_0 = 6.4$ m, $h_1 = 3.2$ m, $k_1 h_1 = 0.167$, and $\alpha = 2$: along (a) x-axis; (b) y-axis.
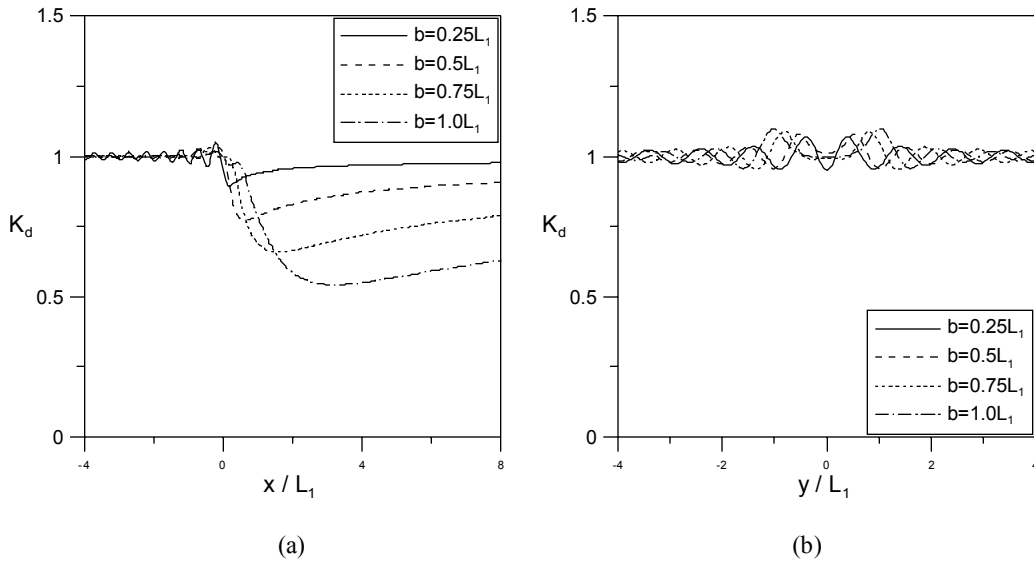

(a)   (b)

Fig. 10. Same as Fig. 9 except for $k_1 h_1 = 1.336$.

27

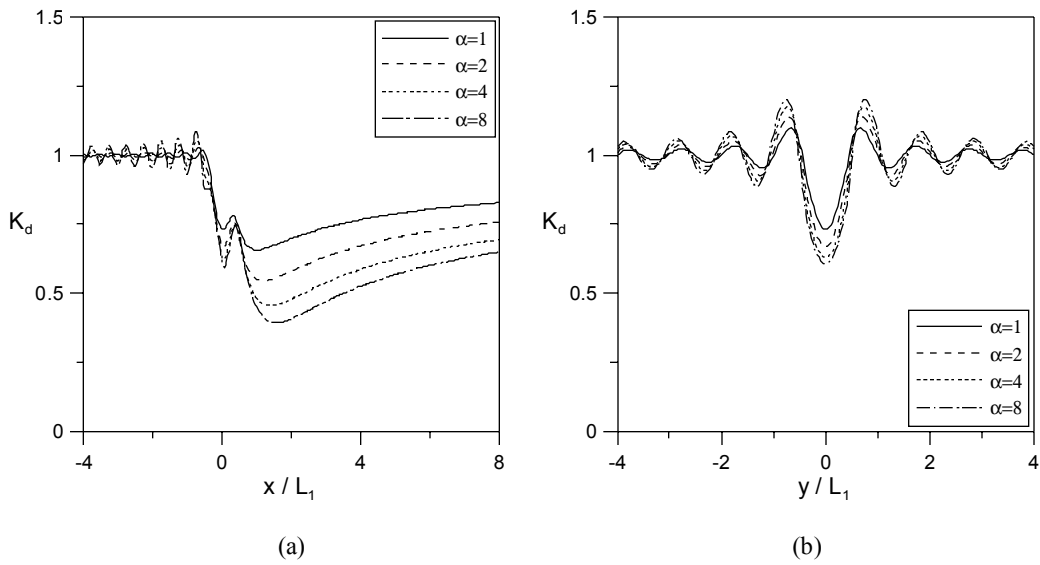|	
(a)	(b)

Fig. 11. Comparison of diffraction coefficients among pits with the same central depth and radius but with different α's and $h_0 = 6.4$ m, $h_1 = 3.2$ m, $b = 0.5L_1$, and $k_1h_1 = 0.167$: along (a) x-axis; (b) y-axis.

(a)	(b)

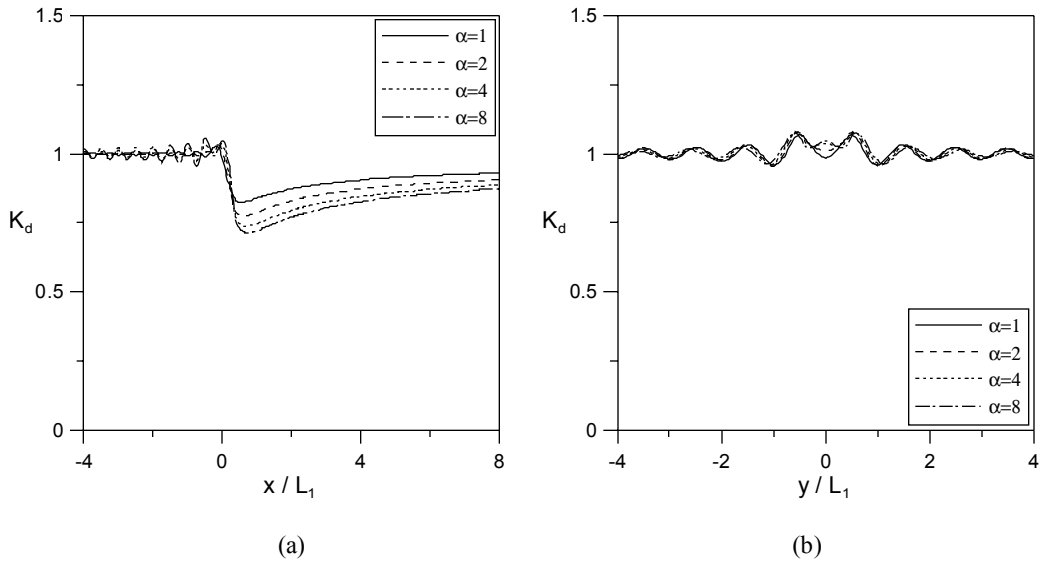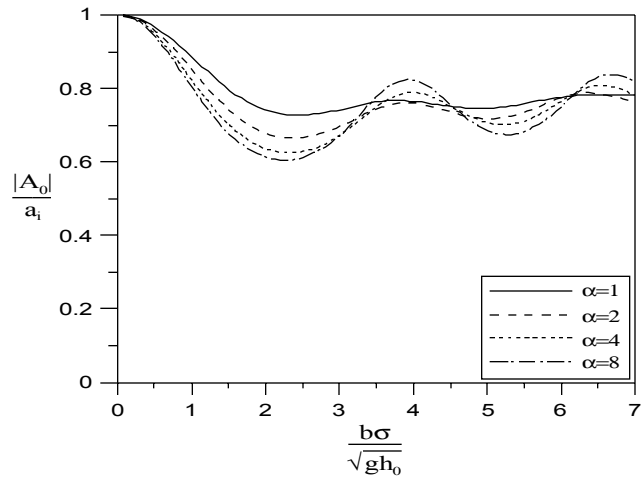Fig. 12. Same as Fig. 11 except for $k_1h_1 = 1.336$.

Fig. 13. Dimensionless amplitudes of the first wave modes in the region of pits with different α's as a function of dimensionless frequency, $b\sigma / \sqrt{gh_0}$.